Proceedings of the 8th International Conference on Fluid Mechanics (ICFM8)
September 25-28, 2018, Tohoku University, Sendai, Japan

Numerical experimental study on flood control function of discontinuous levee system for steep rivers

Hiroshi SENOO [1,*], Tadaharu ISHIKAWA [2]

[1] *Token C.E.E. Consultants Co., Ltd., Tokyo, 174-0004, Japan; email: senoo-h@tokencon.co.jp*
[2] *Tokyo Institute of Technology, Kanagawa, 226-8503, Japan; email: workishikawa0612@yahoo.co.jp*

Abstract: Discontinuous levee systems of various arrangement were constructed for flood control in pre-modern times of Japan when large scale continuous levees could not been realized. The most common levee arrangement, a series of partially overlapped funnel-shaped levees opening upstream, is now collectively called *kasumi* levees, but there was a variety of discontinuous levee systems which did not have levee overlaps along some significantly steep rivers. In this study, the flood control function of those levee systems were investigated by a series of numerical experiments using a shallow flow model on unstructured triangular grid system. Experimental conditions were determined based on the dimensions of old Midai River levee system which was constructed before the 16th century. The calculation results clarified that the levee system of only one meter in height efficiently restricted the transverse inundation expansion up to the flood discharge of 1/30 (/year) in occurrence probability. Furthermore, the results of sensitivity analyses of the flood area to changes in levee opening angle, levee length, and river channel slope, suggested that the arrangement of the discontinuous levees were carefully deliberated to a remarkable extent. Based on the above results, it was concluded that the strategy of flood control of significantly steep rivers in those days was to widen the flood flow safely and effectively by discontinuous, without overlap levees.

Key words: Flood control strategy, Pre-modern times, Numerical experiments, Unstructured triangular grid system.

* Corresponding author. Email: senoo-h@tokencon.co.jp

1. Introduction

In early modern Japan, prior to the middle of the 19th century, large-scale embankments were not built for flood control purposes, and instead, discontinuous levee systems of various arrangement were constructed. The most common arrangement, collectively called *kasumi* (meaning *haze*) levees now, is shown in Figure 1. The hydraulic function of such levees has been described as allowing floodwaters that exceed the river channel capacity to overflow in the upstream direction in order to reduce river discharge levels, and then allowing the stored overflow to drain into the river channel once the floodwaters had receded.

However, Okuma (1987) states that the term *kasumi* levee had been established in modern times, and that the layout and function of actual discontinuous levees may have been more diverse. For example, a study of the Kurobe River conducted by Senoo et al. (2018) showed that the layout of levee openings is closely related to drainage into the former river channel. These results suggest that we may be able to gain a deeper understanding of floodwater control in pre-modern times by studying the hydraulic functions of discontinuous levees located in various rivers, providing that are different from the stereotypical case shown in Figure 1.

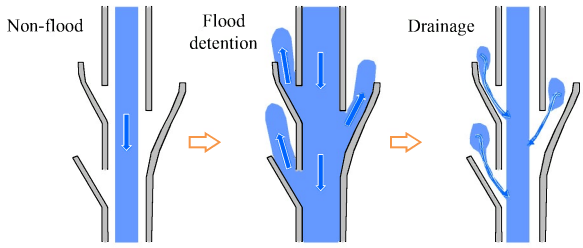

Figure 1. Typical *kasumi* levee arrangement

On rivers with extremely steep slope, some short levees are located at a distance from the river channel so as to have almost no overlapping parts with the channel, as shown in Figures 2(a) and 2(b). These levees have also been considered as a variation of *kasumi* levee, even though their flood control mechanism may have been different from a typical example of the type. In this study, we performed a series of numerical experiments based on shallow water flow equations using a simplified waterway of the pattern shown in Figure 2(a), and then discussed the hydraulic functions of such types of discontinuous levees.

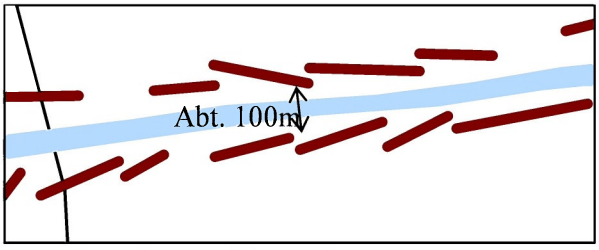

Figure 2(a). Former Midai River levee system of the 15-16th century (Minami-Alps City, 2015)

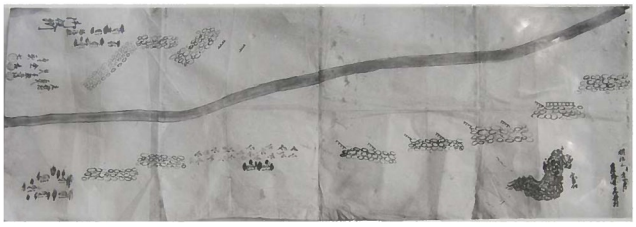

Figure 2(b). Discontinuous levees on the Arakawa River (1870, Fukushima City History Compilation Office archive collection)(Yokoyama et al., 1990)

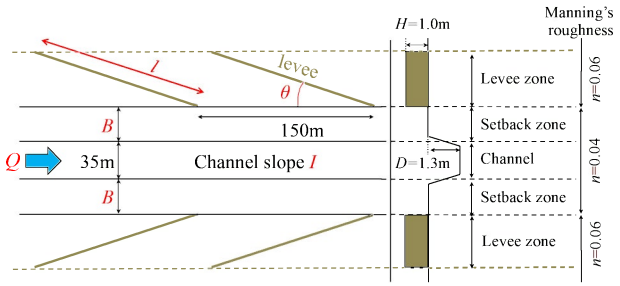

Figure 3. Model of discontinuous levee

Table 1. Various levee properties

Variable	Calculation conditions
θ	10°, **18°**, 30°
l (m)	0 (without levee), 100, **150**
I	**1/50**, 1/80, 1/100
B (m)	0, **30**
Q (m^3/s)	200, **300**, 400, 500

2. Methodology

2.1 Numerical model

A set of shallow water equations was adopted for the numerical simulation model.

$$\frac{\partial h}{\partial t}+\frac{\partial (Uh)}{\partial x}+\frac{\partial (Vh)}{\partial y}=0 \tag{1}$$

$$\frac{\partial (Uh)}{\partial t}+\frac{\partial (UUh)}{\partial x}+\frac{\partial (UVh)}{\partial y} = -gh\frac{\partial H}{\partial x}+\frac{\partial (h\tau_{UU})}{\partial x}+\frac{\partial (h\tau_{UV})}{\partial y}-\frac{\tau_0}{\rho}\frac{U}{\sqrt{U^2+V^2}} \tag{2}$$

$$\frac{\partial (Vh)}{\partial t}+\frac{\partial (UVh)}{\partial x}+\frac{\partial (VVh)}{\partial y} = -gh\frac{\partial H}{\partial y}+\frac{\partial (h\tau_{UV})}{\partial x}+\frac{\partial (h\tau_{VV})}{\partial y}-\frac{\tau_0}{\rho}\frac{V}{\sqrt{U^2+V^2}} \tag{3}$$

where (U, V) are the velocity components in (x, y) coordinates, h is the water depth, H is the water surface level (= h + ground level), ρ is the water density, and g is the gravitational acceleration. τ_0 is the bed friction force, and τ_{UU}, τ_{UV} and τ_{VV} are the horizontal shear stresses, which are expressed by the following equations:

$$\tau_0=\rho U_f^2=n^2\frac{\rho g(U^2+V^2)}{h^{1/3}} \tag{4}$$

$$\tau_{UU}=2\varepsilon\frac{\partial U}{\partial x}-\frac{2}{3}k \quad \tau_{UV}=\varepsilon\frac{\partial U}{\partial y}+\varepsilon\frac{\partial V}{\partial x} \quad \tau_{VV}=2\varepsilon\frac{\partial V}{\partial y}-\frac{2}{3}k$$

$$\varepsilon=\frac{1}{6}\kappa U_f h \qquad k=2.07U_f^2$$

where U_f is the friction velocity, n is Manning's roughness coefficient, ε is the vertically averaged eddy viscosity, k is the turbulent kinetic energy, and κ is the Karman constant.

The differential equations were converted to difference equations by the finite volume method on the unstructured triangular mesh system. The equation forms and solving process are described in Akoh et al. (2017).

The flow rate over the banks was calculated by the formula presented by Honma (1940):

$$q=\begin{cases}0.35\,h_1\sqrt{2gh_1} & if\ h_2/h_1\le 2/3\\ 0.91\,h_2\sqrt{2g(h_1-h_2)} & otherwise\end{cases} \tag{5}$$

where q is the flow rate over the unit length, and h_1 and h_2 are the water depths on the upstream and downstream sides, respectively.

2.2 Experiment conditions

The model of discontinuous levees shown in Figure 3 was placed along the center line of an experimental flume, which was set at 1,900 m long with a width of 600 m. A 35-m-wide and 1.3-m-deep waterway was set at the center. The waterway had funnel-shaped levees opening upstream at a setback B from the riverbank and regularly arranged at 150 m intervals. The levee length is l, the opening angle at a side is θ, and the riverbed slope is I. The levee height was set at 1 m based on survey data from local municipalities (2015). The values for θ, l, I, and B used in the numerical experiments are shown in Table 1. The underlined values in

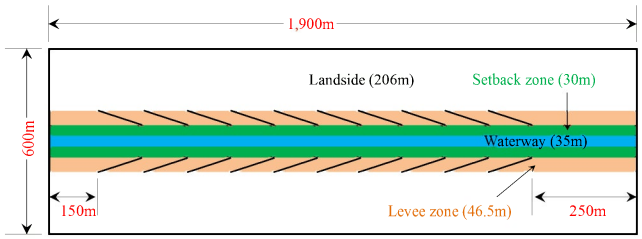

Figure 4. Levee arrangement in the standard pattern

the table are the mean values for the former Midai River (Figure 2(a)), and the combination of these values was taken as the standard pattern. In the following discussions, note that the term "levee zone" refers to the section with levees, "setback zone" refers to the space between the waterway and the levee zone, and "landside" refers to the area on the outside of the levee zone.

Figure 4 shows the layout of waterway and levees in the standard pattern. Here, we can see 10 funnel-shaped levees laid out after a 150 m approach section. A constant discharge was allowed to flow into the upstream end of the regular waterway while the downstream end was set to a free runoff condition, and the flow conditions after attaining a steady state were studied. Based on hydrological data for the water systems including Midai River, the hydraulic conditions for numerical experiment were assumed 200, 300, 400, and 500 m^3/s, as shown in the bottom line of Table 1. These discharge rates correspond to occurrence probabilities of 1/3.3, 1/8, 1/14, and 1/30 respectively.

3. Flow structure in the standard pattern

Figures 5(a) to 5(d) are color contour maps of inundation depth for each discharge rate in the standard pattern. When Q = 500 m^3/s is reached, the width of floodwater at the approach section goes beyond the outer edge of the levees, although the water recedes to the levee zone by the second set of levees and continues to flow with the same repeated pattern thereafter (i.e., quasi-equivalent flow state) inside the levee zone.

Water depth along the levees is lower than the levee height (one meter) until Q = 400 m^3/s, but by Q = 500 m^3/s, the water is slightly over it at the inner edge of the levees. However, the depth of levee overtopping is still a few centimeters, and the risk of levee damage can be considered small. Although the occurrence probabilities of the abovementioned discharge rates are not absolute, if we assume that these are the standard for consideration, then the flow capacity of the former Midai River discontinuous levees has a sufficient capacity for controlling flood flow of an occurrence probability of about 1/8 and may possibly have been capable of maintaining flood flow control for probabilities up to about 1/30.

Figures 5(e) and 5(f) show the results of calculation without levees. The flood overflow expands in a parabolic

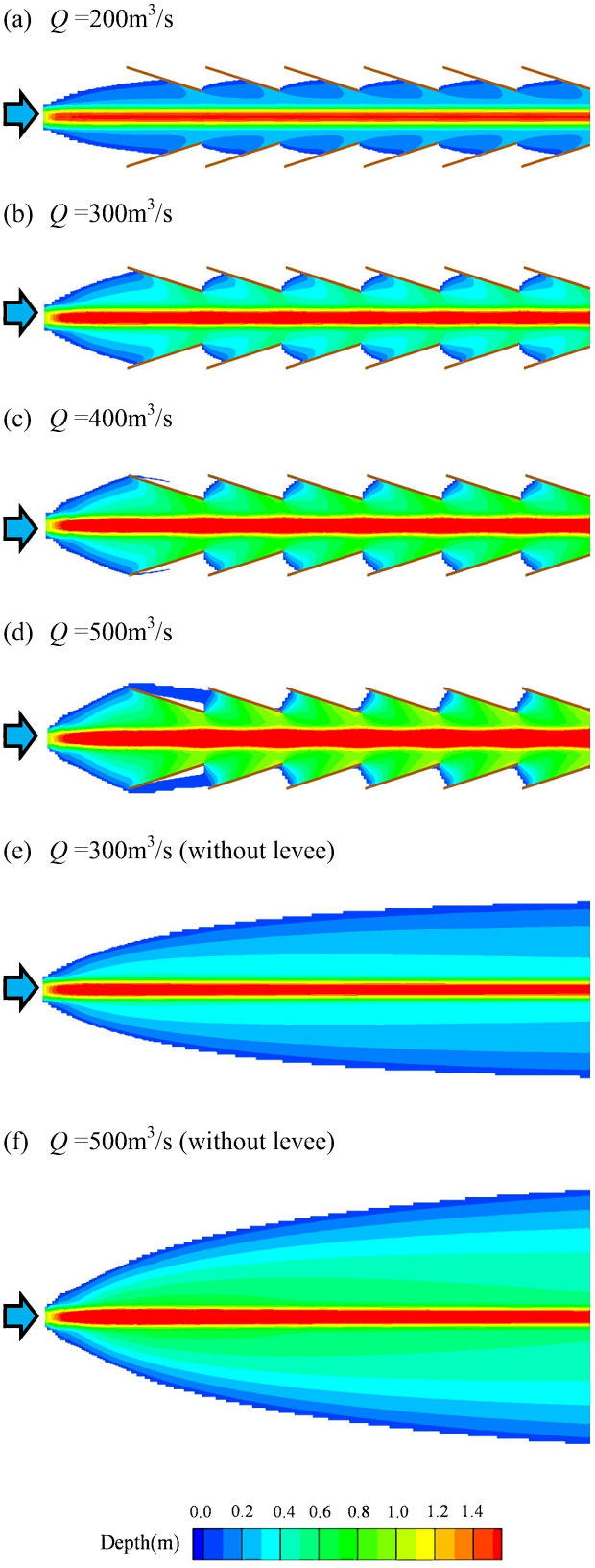

Figure 5. Water depth distribution calculated for the standard pattern

(a) Q =300m^3/s (water depth distribution)

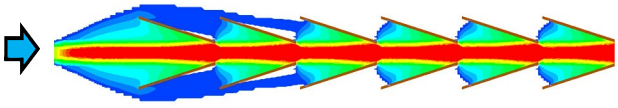

(b) Q =500m^3/s (water depth distribution)

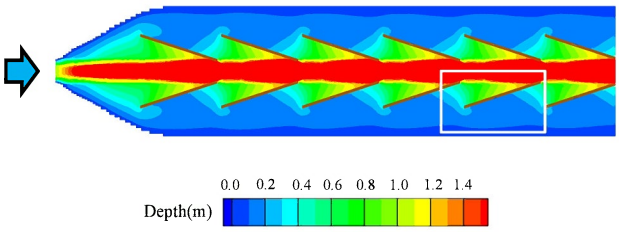

(c) Q =500m^3/s (magnified flow velocity distribution of the boxed area in (b))

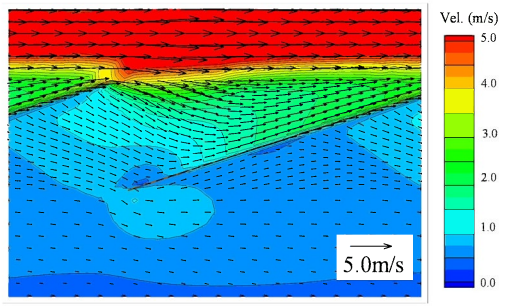

Figure 6. Water depth distribution calculated for the case without setback zone

(a) θ=10° (Q =300m^3/s)

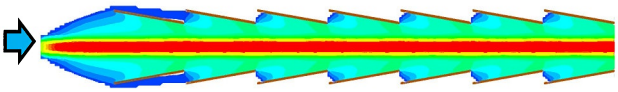

(b) θ=10° (Q =500m^3/s)

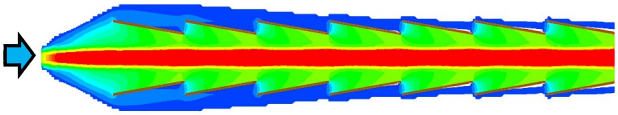

(c) θ=30° (Q =300m^3/s)

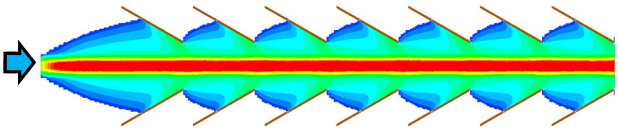

(d) θ=30° (Q =500m^3/s)

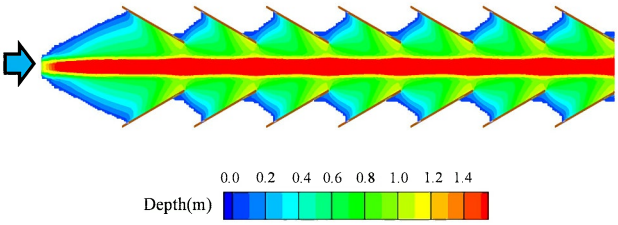

Figure 7. Change in water depth distribution due to the opening angle of the levee

shape, with the expansion rate increasing along with the discharge rate. In a significantly steep river (at I = 1/50 in the calculations), because floodwater flow has extremely high velocity, it may cause serious damage on the landside area and possibly change the river channel on the alluvial fan. In the calculations for (b) and (d) with discontinuous levees for the same discharge rate, although the water slightly overflows near the inner edge of the levees at Q = 500 m^3/s, the water depth is generally quasi-uniform in the levee and setback zones, which effectively narrows down the flood area.

4. Effect of change in levee pattern on flow condition

4.1 Effect of setback

Figures 6(a) and 6(b) show the calculated results for the case without a setback zone (B=0) when Q = 300m^3/s and 500m^3/s. Other parameters were same as the standard values. Comparing them with the cases with a setback zone (Figures 5(b) and 5(d)), the floodwater overflows from the levee zone to the landside. In addition, the water depth near the inner edge of the levees exceeds one meter (levee height). Figure 6 shows the flow velocity distribution for the reach of fifth levee set where the flow became stable. The flow velocity near the inner edge of the levees was over 2 m/s, and the risk of levee collapse may be very large. Therefore, it is considered that the levee setback zone was necessary to increase the levee safety level.

4.2 Effect of opening angle

Figure 7 shows the change in the water depth distribution when the levee opening angle is smaller than (θ = 10°) and larger (θ = 30°) than the standard pattern (θ = 18°). The corresponding calculations for the standard pattern are shown in Figures 5(b) and 5(d). Since the space

(a) Change in water depth (Q =500m^3/s)

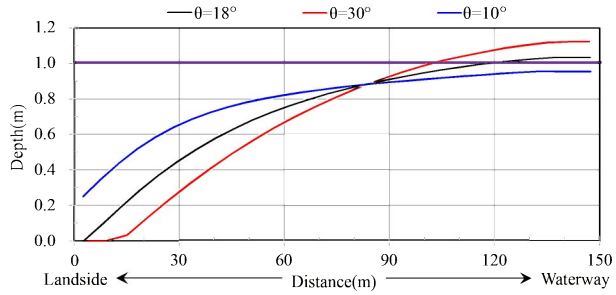

(b) Change in velocity (Q =500m^3/s)

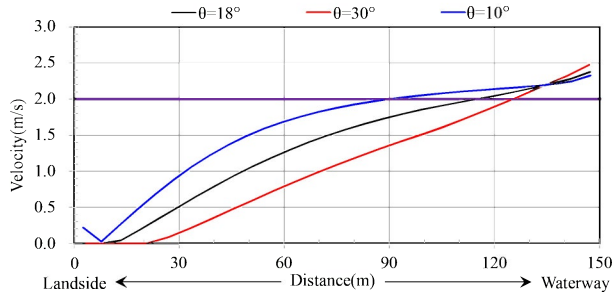

Figure 8. Change in water depth and flow velocity along the levee due to the opening angle

within the funnel shape is narrow for θ = 10°, the water overflows outward from the levee zone at Q = 500 m^3/s. On the other hand, since there is additional space for θ = 30°, flooding to the outer section does not occur, but the water rises in areas where it collides with the levees near the inner edge, thereby causing overflows.

Figure 8 shows a comparison of the water depth and flow velocity (in absolute values) distributions along the levee for opening angles of θ = 10°, 18° (standard), and 30° at Q = 500 m^3/s. The 1 m water depth in Figure 8(a) represents the height of the levee crown. The 2 m/s flow velocity in Figure 8(b), indicated by the reference line, is the criteria of flow velocity for grass turf erosion on levee slopes given by Fukuoka et al. (1990) Since the levee line direction is close to the general flow direction for θ = 10° (indicated by the blue lines), the water level rise is smaller and overflow does not occur even though the flow velocity exceeds 2 m/s for about half the length of the levee. For θ = 30°, the levee exerts a significant drag effect on the flow, which results in overflow and high flow velocity near the inner edge of the levee. A relative comparison of the results above suggests that the flow conditions in the standard pattern (θ = 18°) are the most preferable.

(a) l=100m (Q =300m^3/s)

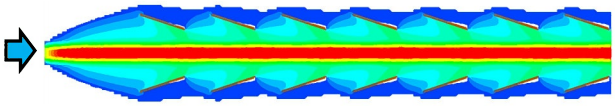

(b) l=100m (Q =500m^3/s)

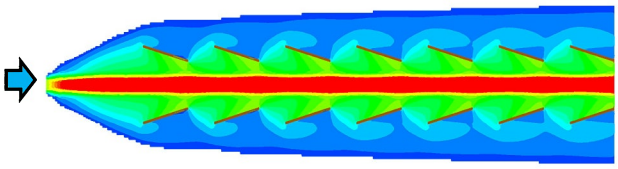

(c) l=200m (Q =500m^3/s)

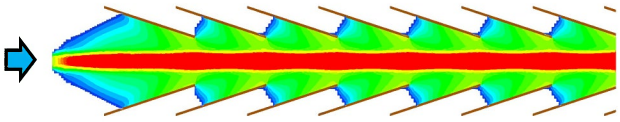

(d) l=200m (Q =750m^3/s)

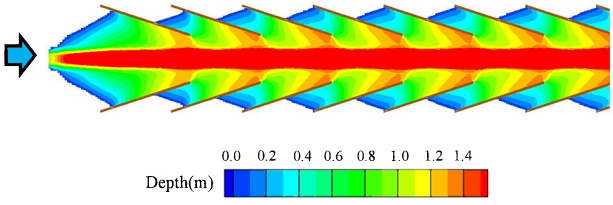

Figure 9. Change in water depth distribution due to levee length

4.3 Effect of levee length

Figure 9 shows the change in the water depth distribution when the levee length is shorter (l = 100 m) than and longer (l = 200 m) than the standard length (l = 150 m). The corresponding calculations for the standard pattern are shown in Figures 5(b) and 5(d). At l = 100 m, the landside is inundated even at a discharge of Q = 300 m^3/s while floodwater did not overflow outward from the levee area even for the discharge rate of Q = 500 m^3/s (Figure 5(d)) This implies that the 50 m difference in levee length has great significance with respect to flood control. When the levee length is extended to l = 200 m, on the other hand, the extra 50 m of levee does not contribute to the flow control at Q = 500 m^3/s. At Q = 750 m^3/s (with an occurrence probability of 1/100), the spaces between the overlapping levees were also inundated and water did not overflow onto the landside. However, since the water inundation overflowed for about 40 cm at the inner edge of

(a) I=1/80 (Q =400m^3/s)

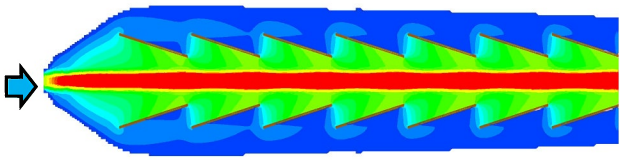

(b) I=1/80 (Q =500m^3/s)

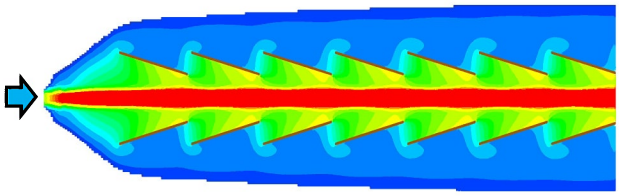

(c) I=1/100 (Q =300m^3/s)

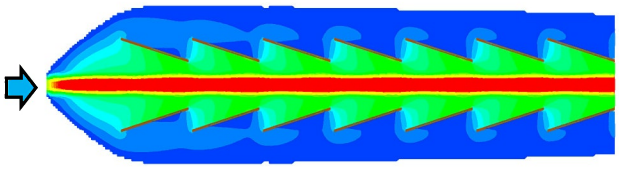

(d) I=1/100 (Q =500m^3/s)

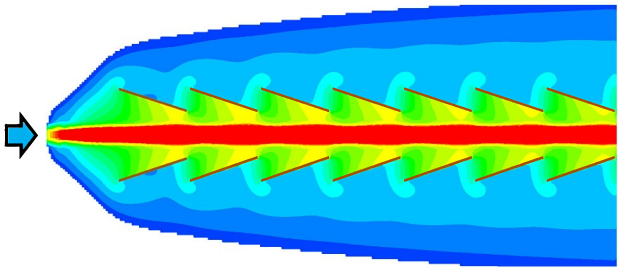

(e) I=1/80 (Q =500m^3/s) l=200m

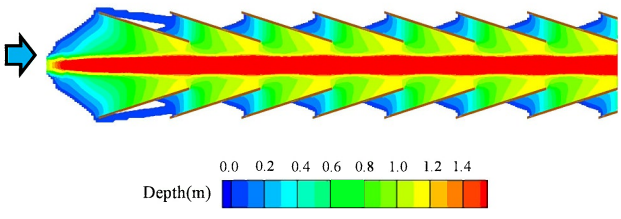

Figure 10. Inundation depth for variation of channel slope

(a) Modern times

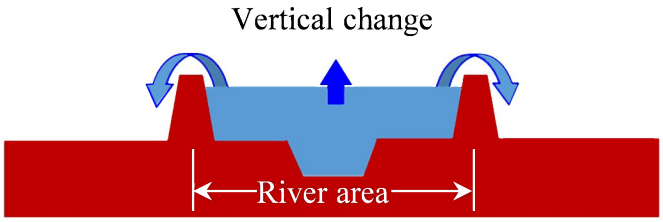

(b) Pre-modern times

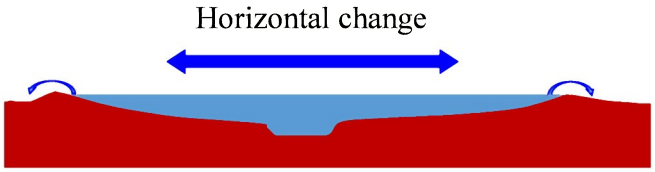

Figure 11. Flood control strategy in modern times and pre-modern times

the levees, there is a high possibility of levee collapse. This implies that in a steep river channel with a slope of 1/50, overlapping levees do not seem to serve any hydraulic purpose.

4.4 Effect of river channel slope

Figure 10 shows the water depth distribution when the river channel slope is smaller (I = 1/80 and 1/100) than the standard slope (I = 1/50). The corresponding calculations for the standard pattern are shown in Figures 5(b), 5(c), and 5(d). At I = 1/80, water overflows into the landside at Q = 400 m^3/s. As previously mentioned, flooding onto the landside not only causes flood damage, it can also change the river channel on the alluvial fan. At I = 1/100, flooding on the landside occurs even at a discharge of Q = 300 m^3/s.

Accordingly, when the calculation is performed with the levee extended to 200 m, as shown in Figure 10(e), even the overlapping sections of the levees are inundated, thereby alleviating overflow into the landside. This implies that making the levees overlap, as in typical *kasumi* levees, starts to serve a purpose when the terrain slope is sufficiently small.

5. Discussion

In current river channel design, the flood is confined within the river channel by constructing sufficiently high levees and dredging low waterways. As a result, the cross section of river channels during floods enlarges vertically (Figure 11(a)). However, once flood discharge exceeds the bankfull discharge, levee overtopping collapses earth levees and generates a stream of destructive power on the floodplain because of the difference in water elevation across the bank. This sudden transition from a state of safety to serious danger is the reason for the recent debates

on how to counter floods that exceed the design flood discharge.

On the other hand, the levee height in pre-modern times was 3 m at most even in large rivers, and that at small scale steep river channel such as Midai River was merely 1 m high. Thus, the flood flow cross-sectional area often had to be enlarged horizontally. This pattern may be considered as the basis of pre-modern river technology (Figure 11(b)). The increase in horizontal cross-sectional area would mean more frequent flooding occurrences according to the modern way of thinking, but people in pre-modern times anticipated that flood areas would expand, and accordingly they responded through land use planning. Given this background, the numerical experimental results obtained in this study can be summarized and the design philosophy of discontinuous levees constructed in Midai River (Figure 2(a)) and Fukushima Prefecture's Arakawa River (Figure 2(b) can be inferred as discussed below.

The aim of discontinuous levees was to widen the flood flow safely and effectively without catastrophic damage to villages. In steep rivers on alluvial fans, a shift of the river channel in the lateral direction may have caused serious flood damage. This means that the range of the flood area had to be restricted while the flow cross-sectional area was enlarged. This suggests that discontinuous levees without overlapping sections, in combination with levees shorter than typical *kasumi* levees, may have served to maintain a uniform flooding depth and effectively suppress the lateral shift of rapid river currents. Moreover, levee setback zones from the regular waterway alleviated flow impact on the inner edge of the levee, as shown in Figure 6. Although the Midai River levees were just 1 m high, they may have controlled floods with occurrence probabilities up of 1/30. The results of sensitivity analyses of the flood area with respect to changes in levee opening angle, levee length, and river channel slope, suggest that the properties and arrangement of the discontinuous levees were carefully deliberated to a remarkable extent.

6. Conclusions

We reported on the results of our study into the hydraulic functions of discontinuous levees constructed for very rapid river currents through numerical experiments using the properties of the former Midai River levees. However, since there were many assumptions concerning the simplification of topography and discharge scale, further discussions on the similarities between the actual considerations on flood control by river engineers in those times and the conclusions obtained from the numerical experiments will be necessary. Nevertheless, summarizing the hydraulic studies of early modern flood control performed by the authors (Ishikawa et al.; 2016, Ishikawa et al.; 2017, Senoo et al. 2018) it is likely that river engineers in pre-modern times had fully mastered the available technology needed to safely expand and restrict flood flow areas.

With such a flood control policy, it seems that a variety of discontinuous levees were conceived based on the conditions of the relevant river basins. Accordingly, stereotyping of discontinuous levees in pre-modern times, *kasumi* levees, may cause researchers to lose sight of the essential ingenuity of pre-modern flood control methods. Both discontinuous levees built for very steep rivers with a slope larger than 1/100 and typical *kasumi* levees have a resemblance of a successive arrangement of funnel-shaped levees opening upstream. However, the former did not have overlapping sections, which were unnecessary because of the high inertia of flow.

References

Akoh, R., Ishikawa, T., Kojima, T., Tomaru, M. and Maeno, S. 2017. “High-resolution modeling of tsunami run-up flooding: a case study of flooding in Kamaishi city, Japan, induced by the 2011 Tohoku tsunami”, *Natural Hazards and Earth System Sciences*, 17, pp.1871-1883.

Fukuoka, S. and Fujita, K. 1990. “Erosion Limit of Sod on the Slope of Levees”, *Journal of Hydraulic Engineering* , 34. pp.319-324.

Honma, H. 1940. “Coefficient of flow volume on low overflow weir”, *Journal of Japan Society of Civil Engineers*, 26, pp.635-645.

Ishikawa, T. and Akoh, R. 2016. “Estimation of flood risk management in 17th century on Okayama Alluvial Plain, Japan, by numerical flow simulation”, *J. of Safety and Security Eng.*, Vol. 6, No. 3, pp.455-465.

Ishikawa, T. and Akoh R. 2017. “Estimation of flood risk management on the lowland of Tokyo Area in 17th century by numerical flow simulation”, *4th Int. Symposium of Shallow Flows, Eindhoven*.

Minami-Alps City, 2015. *Maemidaigawa Teibousigun excavation report*, pp.13-14.

Okuma, T., 1987. “A study on the function and etymology of open levee”, *Historical Studies in Civil Engineering*, 7, pp.259-266.

Senoo, H. and Ishikawa, T., 2018. “Estimation of flood control function of *kasumi* levee system on the Kurobe alluvial fan in the Edo era by numerical flow simulation”, *Journal of Japan Society of Civil Engineers*, Ser. B1(Hydraulic engineering), 74, 4, pp.1411-1416.

Yokoyama, K., Itou, N., Mizugoshi, T. and Hatai G. 2008. “Historical *kasumi* levee system along the Arakawa river”, *Japan Society of Civil Engineers 2008 Annual Meeting* , 63-4, pp.189-190.